Progress in Organic Coatings 77 (2014) 1799–1806

Contents lists available at ScienceDirect

Progress in Organic Coatings

journal homepage: www.elsevier.com/locate/porgcoat

Study of the degradation of hybrid sol–gel coatings in aqueous medium

M.J. Juan-Díaz [a], M. Martínez-Ibáñez [a], M. Hernández-Escolano [b], L. Cabedo [b], R. Izquierdo [b], J. Suay [b,*], M. Gurruchaga [a], I. Goñi [a]

[a] Facultad de Ciencias Químicas, Universidad del País Vasco, P. M de Lardizábal 3, San Sebastián 20018, Spain
[b] Departamento de Ingeniería de Sistemas Industriales y Diseño, Universidad Jaime I, Av. Sos Baynat s/n, Castellón 12071, Spain

ARTICLE INFO

Article history:
Received 15 October 2013
Received in revised form 16 April 2014
Accepted 8 June 2014
Available online 16 July 2014

Keywords:
Sol–gel hybrid coatings
Chemical composition
Degradation kinetics

ABSTRACT

The design and development of suitable multilayered functional coatings for delaying corrosion advance in metals and become controlled-release vehicles requires that the properties of the coatings are known. Coatings prepared by the sol–gel method provide a good approach as protective layers on metallic surfaces. This kind of coating can be prepared from pure chemical reagents at room temperature and atmospheric pressure, with compositions in a very wide range of environmentally non-aggressive precursors. Sol–gel coatings based on siloxane bonded units were prepared, starting with an organic–inorganic hybrid system. Synthesis procedures included acid-catalysed hydrolysis, sol preparation, and the subsequent gelation and drying. The alkoxide precursors used were methyl-triethoxysilane (MTMOS) and tetraethyl-orthosilicate (TEOS) in molar ratios of 10:0, 9:1, 8:2 and 7:3. After determination of the optimal synthesis parameters, the materials were characterised by solid ^{29}Si nuclear magnetic resonance (^{29}Si NMR), Fourier transform infrared spectroscopy (FTIR), contact angle measurement and electrochemical impedance spectroscopy (EIS) test. Finally, the materials were assayed by controlling their weight in contact with water, to determine their ability to degrade by hydrolysis. Electrochemical analysis reveals the formation of pores and water uptake during the degradation. The quantity of TEOS is one of the principal parameters that determine the kinetics of degradation. There is a correlation between the degradation process obtained for long periods and the electrochemical parameters obtained by EIS in short times. The study tries to incorporate knowledge that can be used for designing the degradation process of the functional coatings and to control their properties in short times.

1. Introduction

The use of *sol–gel* coatings as replacements for chromate conversion coatings in the pre-treatment for different metallic alloys has become widespread in the past decades. *Sol–gel* coatings have several advantages, e.g., they are an environmentally friendly technology. Another important feature is the good adherence obtained between the metallic surface and the *sol–gel* film, which is based on the establishment of chemical bonding (M—O—M) from the condensation reactions between metal hydroxyls (M—OH) and alkoxide hydrolysable groups (commonly Si—OH) [1].

Additionally, these sol–gel materials are biodegradable and bioerodible leaching non-toxic degradation products [2]. Since sol–gel technology uses a relative low temperature during formation of the inorganic matrix, various organic, inorganic and biological molecules can be introduced as dopant agents with no degradation risk. For these reasons, sol–gel materials have been extensively used as controlled-release matrices [2–5].

Using sol–gel technology, organic–inorganic hybrid materials can be prepared by a silane precursor containing an organic group. Thus, silica gel obtained by the *sol–gel* technology is an inorganic or hybrid (organic–inorganic) polymer produced synthetically by the controlled hydrolysis and condensation of alkoxysilanes. The synthesis of sol–gel silica occurs from liquid precursors *sol* via the initial formation of *wet* gels, in which the inorganic network is surrounded by solvent, which are later removed to yield a dry material. Depending on the organic group present in the alkoxysilane, the hybrid character of the final material will be defined. In contrast to common glass, which is a viscous fluid obtained by the high temperature fusion of SiO_2, *sol–gel* silica is an amorphous, porous material, which is synthesised in mild conditions [6,7].

* Corresponding author. Tel.: +34 964 728192.
E-mail address: suay@uji.es (J. Suay).

http://dx.doi.org/10.1016/j.porgcoat.2014.06.004
0300-9440/

The use of organofunctional silanes as precursors leads to the formation of an organically modified hybrid that improves the flexibility and density of the films and, additionally, gives functionality to the coating so that it is compatible with the subsequent paint system [8–11]. Nevertheless, the characteristic porosity exhibited by these films leads to worse anticorrosive properties, mainly in the long term [12–15]. However, these materials have several attractive features when compared to inorganic sol–gel (e.g. hydrophobicity and durability) [5] and provide a versatile way to prepare modified sol–gel coatings that can be easily applied to implant surfaces.

Finally, the influence of the initial alkoxysilanes selected (the composition of the precursors) in the degradation of the material has not yet been studied in depth. Aspects such as the type of alkoxysilane used or the organic content in the final silicon network can define the material capacity to degrade [8]. Depending on the degradation kinetics the design of the coating system will need to be done by the incorporation of layers able to reduce the permeability to the electrolyte.

The present study reports the synthesis via sol–gel method of hybrid (silica and organic chains) networks with a mixture of two alkoxysilanes MTMOS and TEOS, which can be used as functional coatings. MTMOS alkoxysilane provides an organic character (a methyl group) to the network, while TEOS increases crosslinking kinetics [16]. Different molar proportions MTMOS:TEOS were used. The aim of the work is to investigate how changes in the %TEOS in the hybrid network influence on the degradation of the matrix. In order to characterise the network formation, a spectroscopic study was performed by FTIR and RMN. Moreover, EIS technique was used to study the initial pore structure of the materials and further changes in the coating because of degradation, fundamentally assessing its capacity to resist pore formation and water uptake, recording both parameters as a function of time. Finally, the results of the weight loss in contact with water are reported and correlated with the physicochemical properties of the different networks.

2. Experimental

2.1. Materials

2.1.1. Sol–gel synthesis

Organic–inorganic hybrid coatings were synthesised from MTMOS (Sigma–Aldrich) and TEOS (Sigma–Aldrich). Coatings with different MTMOS:TEOS molar ratios were prepared 10:0 (10M:0T); 9:1 (9M:1T); 8:2 (8M:2T); 7:3 (7M:3T). To ensure a miscible solution of the silane precursors, 2-propanol (Sigma–Aldrich) was used as a co-solvent, in a volume ratio of alcohol:precursor 1:1. A stoichiometric amount of water acidified with HNO_3 (pH = 1), was added as the catalyst of the reaction. After the addition of the catalyst, solutions were stirred for 1 h and set for another hour at room temperature before their deposition on a substrate. This period of time (2 h) is necessary to ensure the maximum extent of the hydrolysis of the methoxy groups of MTMOS and the ethoxy of TEOS.

2.1.2. Sol–gel coatings

Two types of samples were obtained in order to characterise the coatings: those deposited on a metal substrate and those without a substrate, a free film material.

Stainless steel AISI 316-L plates (5 cm × 5 cm, RNSinox, S.L.) were used as a substrate for *sol–gel* deposition. The plates were cleaned with acetone to remove impurities and oil. A dipping device (KSV instrument-KSV DC) with a controlled withdrawal speed was used for the film deposition. Plates were immersed into the dissolution at a speed of 100 cm min^{-1}, left for 1 min and the plates were then removed at the same speed.

Table 1
Thermal treatment applied to obtain the final material.

Material	MTMOS	TEOS	MTMOS:TEOS
Cure temperature (°C)	100	50	80
Cure time (min)	120	120	120

In order to obtain a free *sol–gel* film, Teflon moulds were used. 3 ml of sol were poured into the mould to obtain a homogeneous final film.

The coatings were dried and cured using the thermal process described in Table 1. Curing conditions were previously established by means of the NMR spectroscopy, to ensure the maximum cross-linking, and SEM to prove that the film obtained was homogeneous and free of cracks [5]. During the thermal treatment, the condensation of the remaining OH groups was promoted and evaporation of the solvents occurred, resulting in the final network.

2.1.3. Chemical characterisation

^{29}Si NMR solid spectroscopy was used to determine the Si—O—Si cross-linking density after curing treatment. For the analysis of samples, the obtained free films were ground into powder. Spectra were recorded on a Bruker 400 AVANCE II WB PLUS spectrometer, equipped with a CP-MAS (cross polarisation magic angle spinning) probe. The powder samples were placed in a rotor sample tube of 4 mm. The sample spinning speed was 7.0 kHz. The pulse sequence used was the Bruker standard, frequency was 79.5 MHz, spectral width was 55 kHz, contact time was 2 ms and delay time was 5 s.

The structure of the hybrid coatings was examined by Fourier-transform infrared (FT-IR) spectroscopy (Model FTIR 6700, NICOLET). Free films of each precursor and the mixtures were prepared. The spectra were recorded on the attenuated total reflectance (ATR) mode and the wavelength range was between 4000 and 400 cm^{-1}.

2.2. Contact angle measurement

The wettability of the coatings was determined by the measurement of the contact angle of deionised water onto the *sol–gel* surface using an automatic contact angle meter (DATAPHYSICS OCA 20 Goniometer). The *sol–gel* coatings were deposited onto stainless steel plates and a sessile drop of 10 μl deionised water was placed on the coating surface. The wettability was determined by the half angle method. The value given is the mean value of at least 11 measurements. For the calculation of contact angle values, a statistical analysis was performed. Mean and standard deviation values were calculated using the one-way ANOVA statistical technique. The error protection method used in this research was the Tukey HSD method and the confidence limit used was 95%.

2.3. Hydrolysis degradation test

The hydrolysis degradation test was performed by soaking the coatings in distilled water at 37 °C, during 9 weeks. The hydrolytic degradation was evaluated by weight loss of the coatings before and after soaking in distilled water during different periods of time. After soaking, the samples were dried in an oven at 37 °C for 24 h and they were weighed. Each data point is the average of three individual measurements.

2.4. Electrochemical impedance spectroscopy (EIS)

Electrochemical impedance spectroscopy tests were carried out on coated samples deposited on a metallic substrate exposed to 3.5% NaCl (by weight) in deionised water for up to 24 h. A three

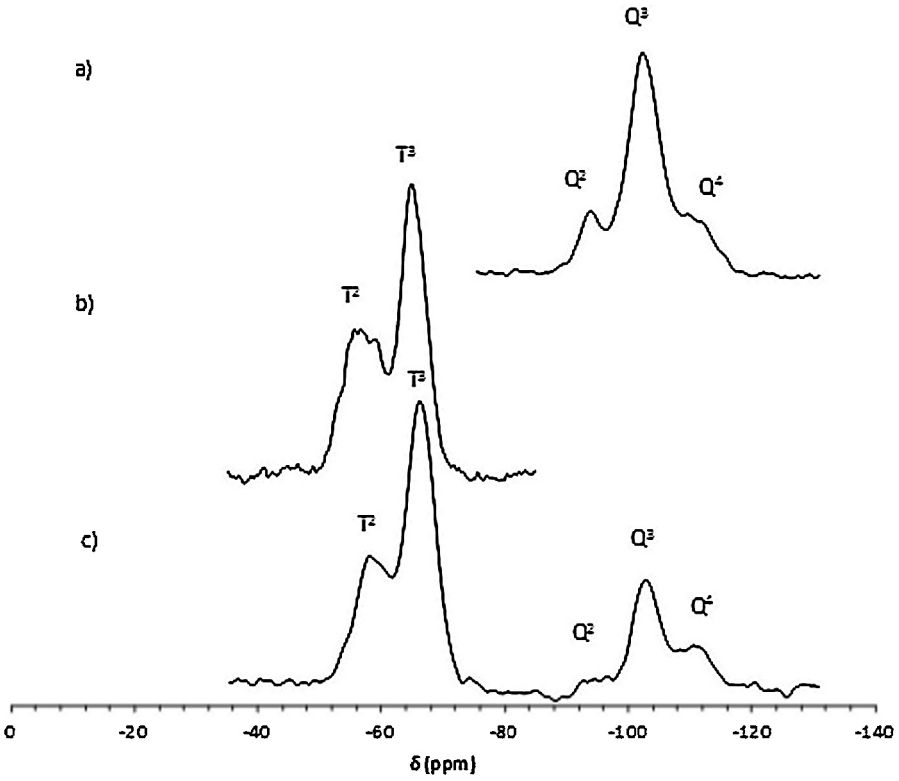

Fig. 1. ^{29}Si solid NMR spectra of (a) TEOS, (b) MTMOS, and (c) MTMOS:TEOS molar ratio 7:3.

electrode electrochemical cell was obtained by sticking a glass cylinder onto the sample sheet and filling it with the test solution.

The exposed surface area was 16.6 cm^2. A carbon sheet acted as the counter-electrode and an Ag/AgCl electrode was used as the reference electrode. The AC impedance data were obtained at the free corrosion potential using an IM6/6eX Zahner—elektrik potentiostat and a frequency response analyser. The impedance tests were carried out over a frequency range of 100 kHz down to 10 mHz using a sinusoidal voltage of 10 mV as the amplitude inside a Faraday cage. This was in order to minimise external interferences on the system.

3. Results and discussion

3.1. Structural characterisation

Following the hydrolysis and condensation of the silane precursors a silica (Si—O—Si) network is formed. The Si—OH bonds obtained by the hydrolysis of the alkoxysilanes will condense to form Si—O—Si bonds. The extent of the condensation reaction will define the network cross-linking density. Different curing treatments were applied in order to obtain homogeneous coatings without pores and those in Table 1 were selected depending on the initial alkoxysilanes mixture.

The free films obtained after the curing treatment were studied by ^{29}Si solid NMR. The nomenclature followed for the description of the condensation degree is extensively described in other papers [17]. Fig. 1 shows the solid state ^{29}Si NMR spectra of TEOS, MTMOS, and 7M:3T, as an example of the mixtures.

^{29}Si NMR solid state spectrum of TEOS coating (Fig. 1a) shows signals associated to Q^2, Q^3 and Q^4 species, where the intensity of $Q^3 \gg Q^2 = Q^4$. The presence of Q^3 and Q^2 species indicates an incomplete condensation process, i.e. either silanol groups or alkoxy groups can be found in the network. However, the intensity of the peak corresponding to Q^3 species together with the presence of Q^4 species shows a high cross-linked material. The MTMOS spectrum (Fig. 1b) shows T^2 and T^3 signals, the relationship between them ($T^3 > T^2$) indicates a high condensation degree of the polysiloxane network, too.

The spectrum of 7M:3T (Fig. 1c) shows T^2 and T^3 species from MTMOS and Q^2, Q^3 and Q^4 from TEOS. Although the presence of T^2, Q^2 and Q^3 species indicates the possibility to have non-reacted Si—OH groups, the relation between the peaks demonstrates that the obtained final network has a high condensation degree. Thus, the addition of TEOS to MTMOS does not affect the cross-linking degree. In Table 2, the ^{29}Si chemical shift (δ) of each species is summarised.

The FTIR assay was used to study the polysiloxane network obtained. Fig. 2 shows the FTIR spectra of the hybrids obtained for MTMOS and 7M:3T.

Both spectra have bands associated with the vibration of chains Si—O—Si around 1075 cm^{-1}, 1163 cm^{-1} and 800 cm^{-1}, which are characteristic of the formation of a polysiloxanic network. The bands associated with the vibration of OH species (3300–3500 cm^{-1}), and Si—OH terminals (3740 cm^{-1}) can be very slightly seen. The bond between the organic chain and the inorganic network Si—C appears at 1450 cm^{-1}. Since the network formed from TEOS precursor is an inorganic network, the introduction into the MTMOS network, gives rise only to a greater amount of Si—O—Si bonds. In both spectra, the band assigned to the vibration of methyl groups of MTMOS at 1275 cm^{-1} was detected.

Table 2
^{29}Si chemical shift (δ) of MTMOS, TEOS and 7M:3T.

Material	δ (ppm)				
	T^2	T^3	Q^2	Q^3	Q^4
MTMOS	−56	−66	–	–	–
TEOS	–	–	−94	−102	−110
7M:3T	−56	−66	−94	−102	−110

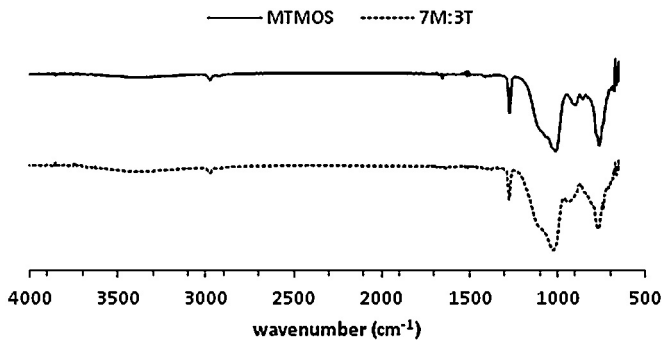

Fig. 2. FTIR spectra (region 4000–400 cm^{-1}) of MTMOS (a) and 7M:3T (b).

The FTIR characterisation has demonstrated that the curing parameters applied to the systems have been correctly selected in order to obtain, in all cases, polysiloxane networks with the presence of methyl organic chains in the materials.

3.2. Wettability

Table 3 summarises the results of contact angle measurements for all the coatings obtained. The MTMOS coating has the smallest hydrophilic character with a contact angle of 76°. The addition of TEOS causes an increase in the hydrophilicity, giving rise to values of around 70° for 30% of TEOS.

Differences in contact angle values can be correlated with the presence of the organic group (methyl) and the content of Si—O—Si bonds in the network. The presence of the methyl group makes the coating less hydrophilic due to the hydrophobic character of this group. On the other hand, the addition of TEOS makes the coatings more hydrophilic due to their increased inorganic character. Additionally, the fact to add TEOS to the MTMOS increases slightly the proportion of more condensed species, which means the elimination of organic groups and hence an increase of the hydrophilicity. Therefore, the design of the hydrophilic–hydrophobic character of the coating can be performed by initially selecting the appropriate mixture of alkoxysilanes.

3.3. Degradation

Sol–gel coatings could degrade in contact with water due to the hydrolysis of the polysiloxane network. It has been established that any form of solid silica in contact with aqueous solutions dissolves into monosilicic acid ($Si(OH)_4$) through hydrolysis, which can be expressed as follows [18]:

$$SiO_2(s) + 2H_2O \leftrightarrow Si(OH)_4 \quad (aq)$$

The weight loss of samples of 10M:0T, 9M:1T, 8M:2T and 7M:3T are presented as a function of immersion time in Fig. 3.

MTMOS coating shows a very low weight loss after 9 weeks of immersion in distilled water, as this coating only lost 1% of its weight. The stable behaviour of MTMOS coating in aqueous medium can be due to the hydrophobic character of the methyl group (Table 3) and to the close polysiloxane network that is formed (Fig. 2), what difficulties water inlet into the network and, as a consequence, the degradation of the network is hindered.

When TEOS is present in the coating formulation a different behaviour is observed. The value of the degradation is dependent on the TEOS content. 9M:1T and 8M:2T coatings show the same trend [5]. Until 3 weeks of immersion in water, they show a fast degradation rate, which is maintained at a constant level until the end of the assay. In contrast, the 7M:3T coating shows a faster initial weight loss, which continues progressively until the end of the assay.

The data indicate that the degradation amount and the kinetics are composition dependent. Coatings with a greater TEOS content show higher degradation values: 18% of weight loss in 9M:1T, 34% in 8M:2T and 57% in 7M:3T (weight loss data after 9 weeks of exposition to water). The degradation results are correlated with hydrophilicity; as TEOS is added to the coating the wettability is higher and the water-flow through the material is favoured. As a consequence, water can produce the hydrolysis of the network, breaking the Si—O—Si bonds.

Additionally, the amount of Si—O—Si bonds is increased when TEOS is added to the coating; thus, the obtained network is more degradable hydrolytically, which is reflected in a higher weight loss.

Table 3
Contact angle measurements for MTMOS and the different molar ratios of MTMOS:TEOS. Values with statistical differences with respect to MTMOS are indicated (*).

Formulation	Wetting contact angle (°)
MTMOS	75.9 ± 1.6
9M:1T	73.2 ± 2.3 *
8M:2T	69.0 ± 0.9 *
7M:3T	70.0 ± 0.8 *

3.4. EIS

The EIS test was performed to study the coating properties (the creation of pores and water uptake) along the time to the electrolyte of MTMOS, 9M:1T, 8M:2T and 7M:3T samples obtained by dip-coating on stainless steel AISI 316L plates.

The impedance spectra were analysed using Z-view software and two different equivalent circuit models, as shown in Fig. 4. The first model has two time constants with the first corresponding to coating behaviour (R_{po} and C_c) and the second corresponding to interphase (R_p and C_{dl}). The second model has three time constants, with the first referred to as the coating response (R_{po} and C_c), the second as the oxide layer (R_{oxid} and C_{oxid}), and the third corresponding to the interphase with metal behaviour (R_p and C_{dl}). The circuit consisted of a working electrode (metal substrate), a reference electrode (Ag/AgCl), electrolyte resistance (R_s), pore resistance (R_{po}), constant phase element of the coating capacitance (CPE_c), oxide layer resistance (R_{oxid}), constant phase element of the oxide layer (CPE_{oxid}), polarisation resistance (R_p) and a constant phase element of the double layer capacitance (CPE_{dl}) [19,20]. The Chi-squared parameter of the fit was always below 0.01. Fitting the EIS data to the circuit determines the values of the characteristic parameters of the equivalent circuit, which are generally assumed to be related to the corrosion properties of the system [19,20]. Fitting the impedance data to the parameters of the first time constant of the circuit (low frequencies) allows the parameters R_{po} and C_c to be obtained. R_{po} can be related to porosity and the deterioration of the coating while C_c is related to the water absorption and coating degradation. R_{oxid} and C_{oxid} are the parameters obtained by fitting the impedance results to the parameters of the second time constant of the circuit (medium frequencies in the case of all three time constants) and referring to the oxide layer properties. Finally, the parameters C_{dl} and R_p are related to the disbonding of the coating and the onset of corrosion at the interface [21–24]. When modelling the equivalent circuit with CPE, the software gives values of capacitance in sn/Ω units together with a parameter known as "*n*". When *n* is close to 1 (ideal capacitor), as was the case in this study, it can be considered that the values of capacitances given by the software match the effective capacitances (ideal).

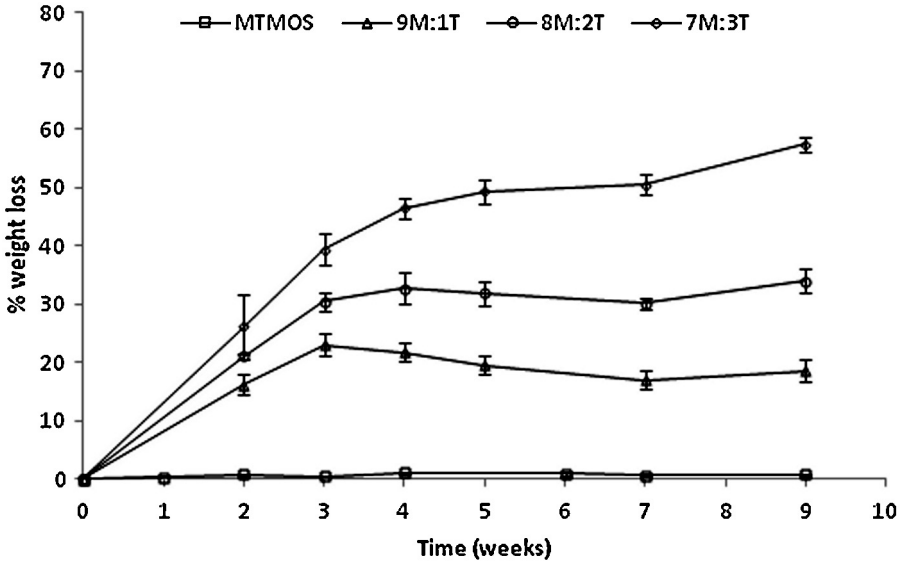

Fig. 3. Weight loss by hydrolytic degradation versus time of immersion in distilled water for MTMOS, 9M:1T, 8M:2T and 7M:3T coatings.

3.4.1. Equivalent circuit interpretation

It is generally assumed that the elements of the equivalent circuits are correlated to the corrosion properties of the system [19,25–30]. Although this is necessary in order to fit correctly the equivalent circuit to all impedance spectra versus frequency, this study is only related to the characterisation of the hydrolysis degradation of the sol–gel coating, and for this reason we will focus our attention to those results obtained at the high frequency where the response of the coating to its exposition to electrolyte (parameters of the equivalent circuit R_{po} and C_c) is located.

The pore resistance R_{po} is a measure of the porosity and deterioration of the coating. R_{po} values have usually been related to the number of pores or capillary channels perpendicular to the substrate surface through which the electrolyte reaches the interface [24]. Although the R_{po} can also increase with immersion time, probably as a result of pore or defect blockage by corrosion products, it usually decreases. Some authors have found three regions in

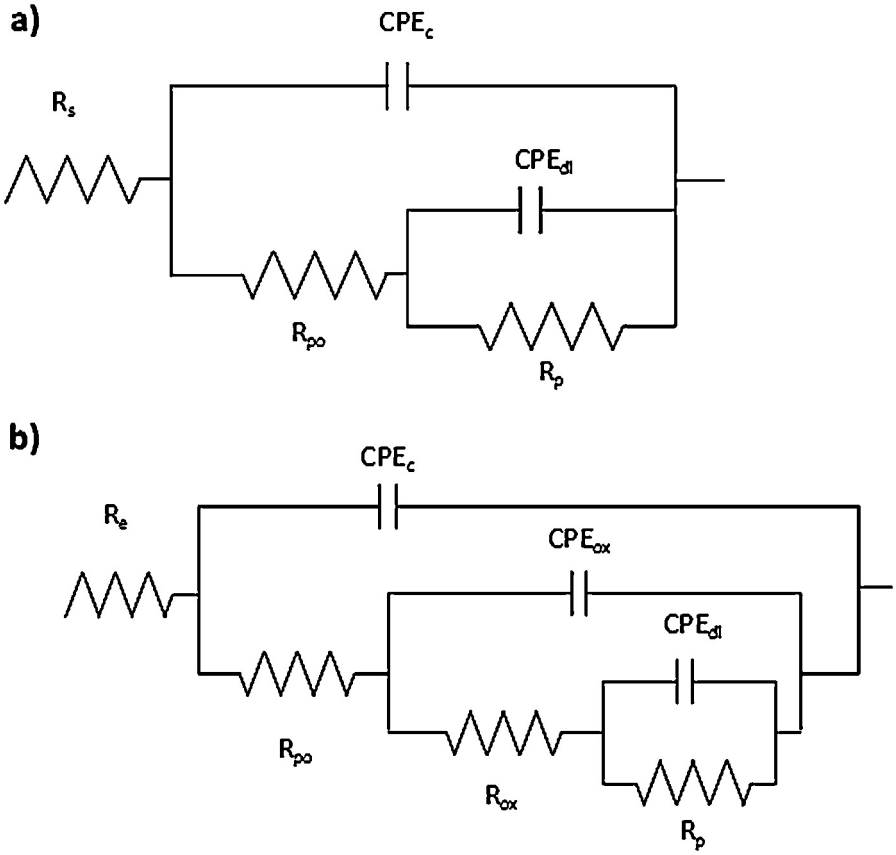

Fig. 4. Equivalent circuit a two time constants and b three time constants.

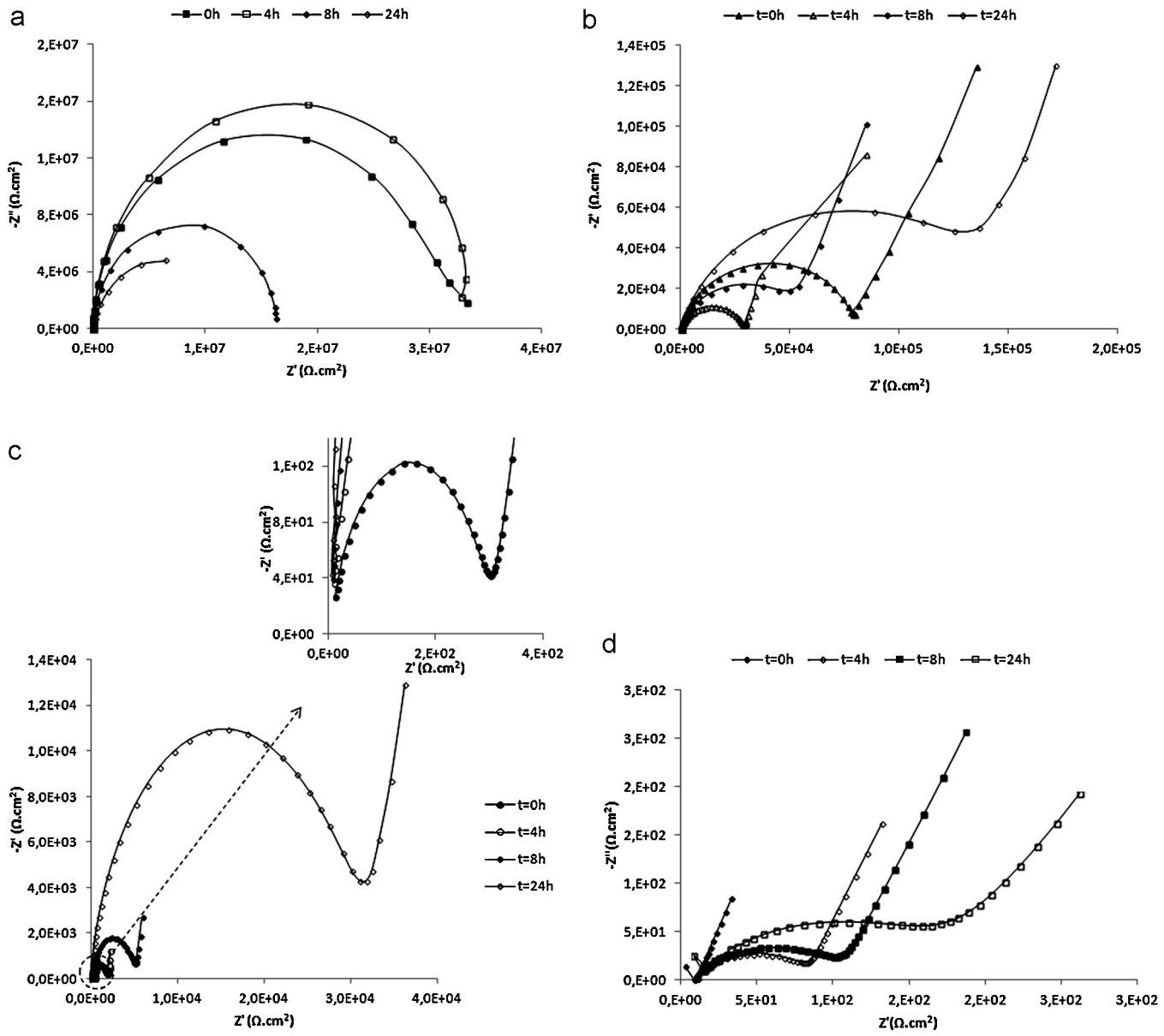

Fig. 5. Evolution of Nyquist plot for (a) MTMOS, (b) 7M:3T, (c) 8M:2T and (d) 7M:3T coatings during 24 h immersion in electrolyte (deionised water 3.5% NaCl by weight).

the time dependent decreases of R_{po}. It initially decreases rapidly, then slowly (displaying a plateau) and then again rapidly, coinciding with the appearance of the second semicircle. They explain the plateau by making the assumption that the number of pathways formed is approximately constant with time. C_c is the capacitance of the coating and it should be a measure of the water permeation into the coating and is given by:

$$C_c = \frac{\varepsilon \cdot \varepsilon_0 \cdot A}{d} \quad (1)$$

where ε is the dielectric constant of the coating, ε_0 is the permittivity of vacuum, A is the area of the coating exposed to the electrolyte, and d is the thickness. The coating capacitance will usually change (increasing) due to electrolyte absorption because the dielectric constant of water is approximately 5 times greater than that of a typical coating. C_c usually increases at the initial stage of exposure, and it is a measure of water absorption. When the coating has been exposed for a long time it can be correlated to disbonding and deterioration.

Fig. 5 shows the Nyquist graph of the impedance evolution with time over the first 24 h for 10M:0T, 9M:1T, 8M:2T and 7M:3T. The impedance spectrum shows that MTMOS' impedance values are bigger than those obtained in coatings with TEOS content. As the quantity of TEOS increases, the impedance module decreases. The exposure to electrolyte has a limited response in the case of MTMOS which means there are not clear changes in the material during the time of the test, while in coatings with TEOS the behaviour is the opposite. There are large changes in the impedance with exposure to electrolytes that would be correlated to the phenomena of degradation.

In order to analyse the behaviour of the coatings, the impedance spectra were modelled using equivalent circuits, as shown in Fig. 5. In the case of MTMOS coatings, only two time constants were detected in the impedance response, while three time constants were detected for coatings in the presence of TEOS. The presence of an oxide layer in the case of TEOS coatings could be due to a higher permeability of these coatings, which was reflected by the significant decrease of the impedance value.

Table 4
Parameter *n* of the CPE elements for each formulation and immersion period used.

Formulation	*n*	0 h	1.5 h	3 h	4 h	6 h	8 h	10 h	24 h
10M:0T	n_1	0.99	0.99	0.99	0.99	0.98	0.98	0.99	0.87
	n_2	0.62	0.66	0.63	0.76	0.88	0.65	0.63	0.85
9M:1T	n_1	1	0.95	0.95	0.94	0.97	0.79	0.79	0.79
	n_2	0.85	0.77	0.75	0.73	0.69	0.82	0.82	0.83
	n_3	0.72	0.8	0.81	0.84	0.82	0.81	0.83	0.86
8M:2T	n_1	0.84	0.85	0.86	0.87	0.88	0.9	0.93	0.89
	n_2	0.86	0.82	0.85	0.81	0.77	0.67	0.62	0.67
	n_3	0.7	0.81	0.81	0.81	0.82	0.82	0.82	0.73
7M:3T	n_1	0.66	0.65	0.63	0.63	0.64	0.61	0.63	0.63
	n_2	0.77	0.86	0.9	0.88	0.88	0.92	0.77	0.77
	n_3	0.8	0.85	0.91	0.89	0.89	0.92	0.75	0.76

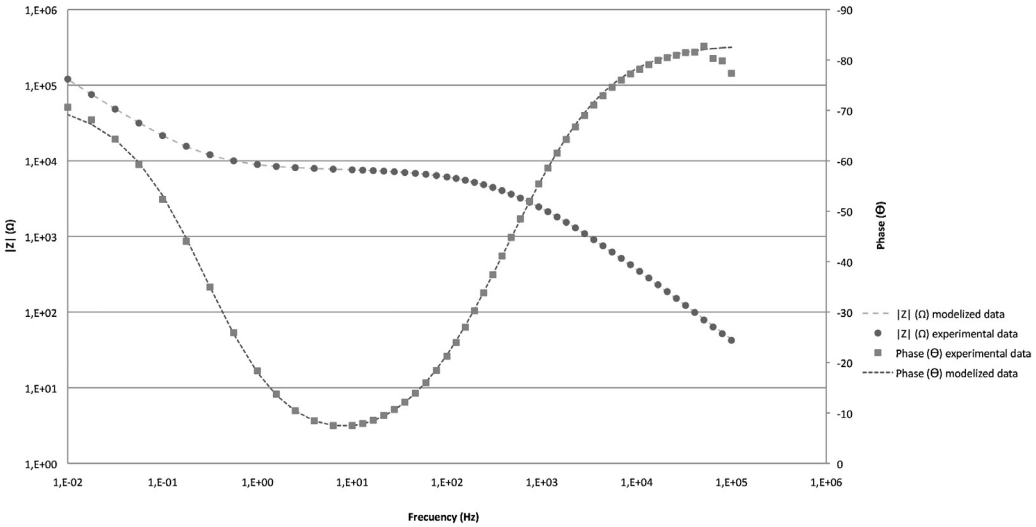

Fig. 6. Bode plot for 8M:2T sample after 10 h in contact with electrolyte. Comparison between experimental data and modelisation results with equivalent circuit.

Impedance experimental results for the coatings were modelled according to the proposed equivalent circuits. As CPE elements were used instead of capacitance elements the values of the parameter n are shown in Table 4, for each formulation and for all the immersion periods used.

Fig. 6 shows both the experimental values and those modelised for sample 8M:2T after 2 h of immersion with the circuit depicted in Fig. 5b.

As this study tried to understand how electrolyte exposure affects the material degradation, the discussion will be focused on the first time constant parameters, which are related to the coating behaviour.

The R_{po} value is a measure of the ionic resistance through the pores of the coatings and is inversely proportional to the extent and number of defects in the coating. The evolution of R_{po} with the exposure time in the electrolyte gives information about the coating capacity to avoid the formation of pores across the film due to its degradation. High and constant R_{po} values are attributed to coatings which do not degrade during electrolyte exposure. Fig. 7 shows pore resistance parameters obtained from the responses of all coatings at high frequencies (10M:0T, 9M:1T, 8M:2T and 7M:3T).

The MTMOS coating shows an initial value of R_{po} of $2 \times 10^7\ \Omega\,cm^2$, and this value remains almost constant until 8 h of contact with the electrolyte, where there is a drastic decrease to a value of $390\ \Omega\,cm^2$ at 24 h of contact. The coating 9M:1T presents an initial value of $28{,}000\ \Omega\,cm^2$ and a final value of $570\ \Omega\,cm^2$. In the case of 8M:2T, the value of R_{po} decreases from $241\ \Omega\,cm^2$ to $8\ \Omega\,cm^2$. Finally, the coating 7M:3T shows an initial value of $20\ \Omega\,cm^2$ and a final value of $49\ \Omega\,cm^2$ after 24 h of contact with the electrolyte.

It can be seen that as TEOS is added to MTMOS coating, the value of R_{po} decreases significantly, especially in the cases of 20 and 30% of TEOS. The 9M:1T coating shows an R_{po} initial value that is three magnitudes less than that of MTMOS, while 8M:2T five magnitudes lower and 7M:3T is six. The addition of 20% and 30% of TEOS makes the coating very permeable to the passage of electrolytes.

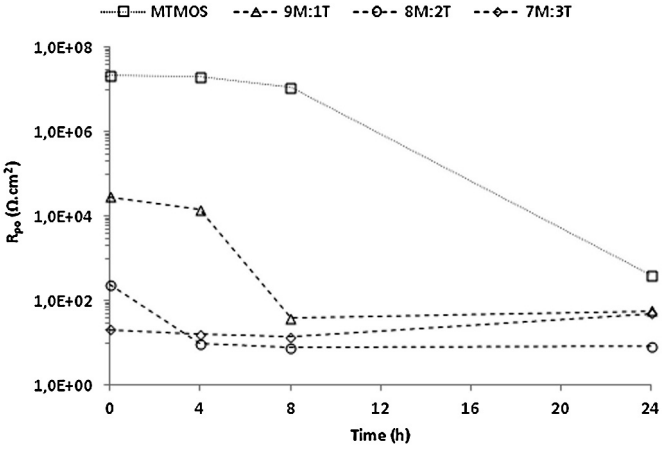

Fig. 7. Evolution of the pore resistance versus time of contact with electrolyte of the coatings MTMOS, 9M:1T, 8M:2T and 7M:3T.

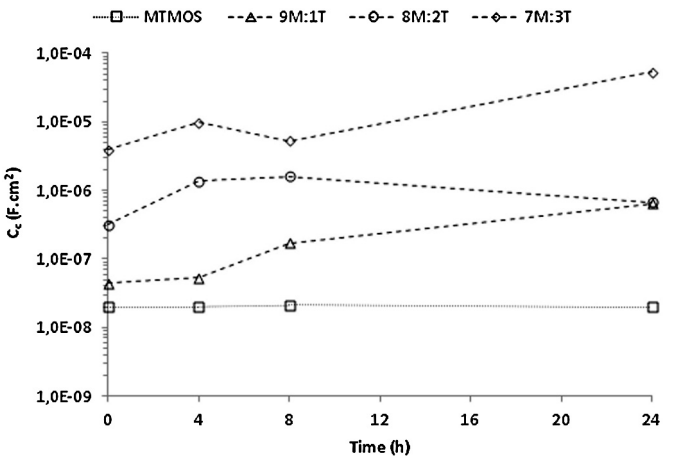

Fig. 8. Evolution of the coating capacitance versus time of contact with electrolyte of the coatings MTMOS, 9M:1T, 8M:2T and 7M:3T.

The increase in the value of C_c can be correlated using Eq. (1) with an increase in the permittivity (ε) value, with the rest of parameters remaining constant for a specific coating sample and test. As a result, an increase of permeability is directly related to an increase in water content in the coating. Fig. 8 shows the coating capacitance parameter obtained from the response at high frequencies of all coatings (10M:0T, 9M:1T, 8M:2T and 7M:3T).

The MTMOS coating shows a constant value of 2×10^{-8} F cm^2, while the rest of the coatings showed upper values for this parameter, which increased with the content of TEOS. The 9M:1T coating shows an initial capacitance value of 4×10^{-8} F cm^2 and a final value of 6×10^{-8} F cm^2, the coating 8M:2T varies the coating value from 3×10^{-7} F cm^2 to 6×10^{-7} F cm^2; and the coating 7M:3T ranks from 4×10^{-6} F cm^2 to 5×10^{-5} F cm^2. In all cases, the final values of C_c are bigger than the initial ones showing that exposure to the electrolyte with time causes the water content to increase in the coatings, and this content is also increased with TEOS content.

These results are in agreement with those obtained by hydrolytic degradation (Fig. 3), where it can be observed that the increase of TEOS content increases the coating degradability. The increase of TEOS increases the permeability of the coating and consequently the water content in them, making the hydrolysis degradation more possible.

Although the addition of TEOS allows obtaining a more cross-linked network due to the appearance of Q^4 species, an increase of species with terminal silanols, as indicated by the presence of Q^2 and Q^3 signals is obtained too. These facts make the network more degradable by hydrolysis. MTMOS:TEOS coatings are more hydrophilic than MTMOS and the parameters R_{po} and C_c show that increase of TEOS causes more channels where the water can penetrate in the coating and cause an increase in their water content.

4. Conclusions

This study demonstrates that changes in the composition of a hybrid *sol–gel* network can strongly affect the degradation of the matrix. NMR results showed that the addition of TEOS is able to increase the network cross-linking density but at the same time this network is more hydrophilic and degradable. The increase of the degradability of the coating can be due to an increased wettability and the amount of siloxane bonds. EIS results showed a big decrease in the pore resistance and an increase in the coating capacitance with the addition of TEOS. The values of the equivalent circuit elements associated to the coating, as the pore resistance and coating capacitance, can be used as an earlier information, obtained in a very short time, of the degradation kinetics in long periods. As a consequence, we can say that as the TEOS content of the coating increases, pore formation across the film is favoured, along with water absorption, which is in accordance with the degradation results obtained. Therefore, the composition of a *sol–gel* coating can be designed in order to obtain a matrix with the desired degradation kinetics changing the chemical compositions of the precursors.

Acknowledgements

The supports of the Ministerio de Economía y Competitividad (Spain) through project IPT-2012-0218-090000 and of the University of the Basque Country (UPV/EHU) through "UFI11/56" are kindly acknowledged. We are especially thankful to D. Antonio Coso and D. Jaime Franco (Ilerimplant S.L., http://www.ilerimplant.com) for their cooperation.

References

[1] V. Palanivel, D. Zhu, O.W.J. van, Prog. Org. Coat. 47 (3–4) (2003) 384–392.
[2] M. Hernández-Escolano, M.J. Juan-Díaz, M. Martínez-Ibáñez, A. Jimenez-Morales, I. Goñi, M. Gurruchaga, J. Suay, J. Sol–Gel Sci. Technol. 2 (64) (2012) 442–451.
[3] I. Goñi, M. Gurruchaga, M.J. Juan-Díaz, M. Martínez-Ibáñez, J. Suay, S. Da Silva, I. Lara-Sáez, J. Franco, A. Coso, Gaceta Dent. 225 (2014) 84–97.
[4] J. Suay, M.J. Juan-Díaz, M. Martínez-Ibáñez, M. Hernández-Escolano, V. Ferrer, J. Franco, A. Coso, I. Lara-Sáez, M. Gurruchaga, I. Goñi, Clin. Oral Implants Res. 23 (Suppl. 7) (2012) 206.
[5] M. Hernández-Escolano, M.J. Juan-Díaz, M. Martínez-Ibáñez, J. Suay, I. Goñi, M. Gurruchaga, J. Mater. Sci. Mater. Med. 24 (2013) 1491–1499.
[6] J. Wright, N. Sommerdijk, The chemistry of sol–gel silicates, in: D. Phillips, S. Roberts (Eds.), Sol–Gel Materials Chemistry and Applications, CRC Press, London, 2001.
[7] J. Wright, N. Sommerdijk, Silica sol–gels: reaction mechanisms, in: D. Phillips, S. Roberts (Eds.), Sol–Gel Materials: Chemistry and Applications, CRC Press, London, 2001.
[8] A. Collazo, M. Hernandez, X.R. Novoa, C. Perez, Electrochim. Acta 56 (23) (2011) 7805–7814.
[9] S. Hofacker, M. Mechtel, M. Mager, H. Kraus, Prog. Org. Coat. 45 (2–3) (2002) 159–164.
[10] N.N. Voevodin, J.W. Kurdziel, R. Mantz, Surf. Coat. Technol. 201 (3–4) (2006) 1080–1084.
[11] D. Wang, G.P. Bierwagen, Prog. Org. Coat. 64 (4) (2009) 327–338.
[12] D. Zhu, O.W.J. van, Corros. Sci. 45 (10) (2003) 2177–2197.
[13] M.L. Zheludkevich, R. Serra, M.F. Montemor, I.M.M. Salvado, M.G.S. Ferreira, Surf. Coat. Technol. 200 (9) (2006) 3084–3094.
[14] N.C. Rosero-Navarro, S.A. Pellice, Y. Castro, M. Aparicio, A. Duran, Surf. Coat. Technol. 203 (13) (2009) 1897–1903.
[15] P. Alvarez, A. Collazo, A. Covelo, X.R. Novoa, C. Perez, Prog. Org. Coat. 69 (2) (2010) 175–183.
[16] M. Hernandez-Escolano, M. Juan-Diaz, M. Martinez-Ibanez, A. Jimenez-Morales, I. Goni, M. Gurruchaga, J. Suay, J. Sol–Gel Sci. Technol. 64 (2) (2012) 442–451.
[17] R.M. Almeida, Atomic scale structure of gel materials by solid state NMR, in: S. Sakka (Ed.), Handbook of Sol–Gel Science and Technology: Processing, Characterization and Applications, 2005.
[18] S. Falaize, S. Radin, P. Ducheyne, J. Am. Ceram. Soc. 82 (4) (1999) 969–976.
[19] S.J. Garcia, J. Suay, Prog. Org. Coat. 57 (4) (2006) 319–331.
[20] S.J. Garcia, J. Suay, Prog. Org. Coat. 66 (3) (2009) 306–313.
[21] A. Amirudin, D. Thierry, Prog. Org. Coat. 26 (1) (1995) 1–28.
[22] G.W. Walter, J. Electroanal. Chem. Interfacial Electrochem. 118 (1981) 259–273.
[23] G.W. Walter, Corros. Sci. 26 (9) (1986) 681–703.
[24] N. Tang, O.W.J. van, G. Gorecki, Prog. Org. Coat. 30 (4) (1997) 255–263.
[25] W.E.P.M. van, G.M. Ferrari, W.J.H.W. De, Corros. Sci. 34 (9) (1993) 1511–1530.
[26] M.T. Rodriguez, J.J. Gracenea, S.J. Garcia, J.J. Saura, J.J. Suay, Prog. Org. Coat. 50 (2) (2004) 123–131.
[27] S.J. Garcia, J. Suay, Prog. Org. Coat. 57 (3) (2006) 273–281.
[28] S.J. Garcia, M.T. Rodriguez, R. Izquierdo, J. Suay, Prog. Org. Coat. 60 (4) (2007) 303–311.
[29] S.J. Garcia, J. Suay, Prog. Org. Coat. 59 (3) (2007) 251–258.
[30] S.J. Garcia, J. Suay, Corrosion 63 (4) (2007) 379–390.